Vol 18 No 12, December 2009
1674-1056/2009/18(12)/5474-05

Chinese Physics B

© 2009 Chin. Phys. Soc.
and IOP Publishing Ltd

Analytical model for reverse characteristics of 4H–SiC merged PN–Schottky (MPS) diodes*

Song Qing-Wen(宋庆文)†, Zhang Yu-Ming(张玉明), Zhang Yi-Men(张义门),
Lü Hong-Liang(吕红亮), Chen Feng-Ping(陈丰平), and Zheng Qing-Li(郑庆立)

Key Laboratory of Wide Band-Gap Semiconductor Materials and Devices, School of Microelectronics, Xidian University, Xi'an 710071, *China*

(Received 21 March 2009; revised manuscript received 19 May 2009)

A new analytical model for reverse characteristics of 4H–SiC merged PN–Schottky diodes (MPS or JBS) is developed. To accurately calculate the reverse characteristics of the 4H–SiC MPS diode, the relationship between the electric field at the Schottky contact and the reverse bias is analytically established by solving the cylindrical Poisson equation after the channel has pinched off. The reverse current density calculated from the Wentzel–Kramers–Brillouin (WKB) theory is verified by comparing it with the experimental result, showing that they are in good agreement with each other. Moreover, the effects of P-region spacing (S) and P-junction depth (X_j) on the characteristics of 4H–SiC MPS are analysed, and are particularly useful for optimizing the design of the high voltage MPS diodes.

Keywords: 4H–SiC, merged PN–Schottky, reverse characteristics, tunnelling current
PACC: 7330, 7340G, 7340N

1. Introduction

Silicon carbide (SiC) is a promising power semiconductor because of its high critical breakdown electric field and high thermal conductivity (∼4.9 W/cmK).[1] These allow a device made from such a material to possess some advantages, i.e. high power capacity, lower series resistance and lower power dissipation.[2] The 4H–SiC merged PN–Schottky diode (MPS or JBS) has shown its attractive properties such as a potential power device. Recently several 4H–SiC merged PN–Schottky diodes (MPS or JBS) have been reported by different groups.[3−5] The MPS is a Schottky rectifier structure with p-n junction grids integrated into the drift region. A schematic of the MPS cross section is shown in Fig.1. The main advantages of the MPS are the Schottky-like on-state and fast switching characteristics together with the off-state characteristics having a lower leakage current similar to that of the PiN rectifier. In SiC, the conduction loss of an MPS can be much lower than that of a PiN diode.[6] The leakage current of MPS is lower than that of conventional Schottky diodes due to the shielding of high electric field from the Schottky contact. This is particularly important for SiC Schottky diodes because the electric field at the SiC Schottky contact is almost one order of magnitude higher than that of silicon Schottky diodes.

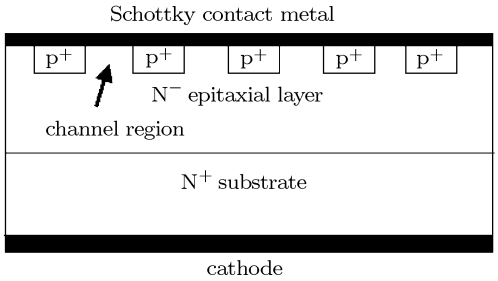


Fig.1. Schematic cross section of the MPS diodes.

Previously, a detailed analysis of the MPS diode has been reported in Ref.[7]. However, this analysis was based on low voltage silicon MPS diodes, so that many assumptions are no longer valid or accurate for the application to the high voltage SiC MPS. Developed in Ref.[8] was a semi-empirical analytical model for the high voltage 4H–SiC MPS with the help of numerical simulation. However, this model cannot express clear physical mechanisms of the MPS. In the present paper, by solving the Poisson equation in the cylindrical coordinate system and using the WKB theory to calculate the reverse current, a new reverse leakage current model for 4H–SiC MPS is proposed.

*Project supported by the Xi'an Applied Materials Innovation Fund (Grant No XA-AM-200702).
†Corresponding author. E-mail: soqwe@126.com

2. Analysis of the reverse characteristics of MPS

When a reverse voltage is applied to the MPS, the depletion layers formed by the p-n junction spread into the channel region under the Schottky contact shown in Fig.1. For an appropriate design, the depletion layers intersect under the Schottky barrier at a relatively low reverse voltage. After the depletion layer pinch-off, a potential barrier is formed in the channel region. Once the potential barrier is formed, further increase of the applied voltage is mainly sustained with the depletion layer extending toward the substrate, and the potential barrier shields the Schottky barrier from the applied voltage. This shielding reduces the electric field at the Schottky contact, resulting in a lower reverse leaking current. However, the electric field at the Schottky contact no longer follows the same trend as the conventional Schottky diodes after the channel has been pinched off. In Ref.[7], the electric field at the Schottky contact was assumed to be kept constant. As a result, the leakage current from thermionic and field emissions would remain unchanged with increasing reverse bias. However, from the experimental results,[5] this assumption is no adequate to accurately model the reverse characteristics of an MPS, particularly for SiC devices of which the electric field is much higher than that of a silicon MPS.

2.1. Reverse leakage current

The basic reverse leakage current mechanisms of MPS diodes are shown in Fig.2. The possible reverse leakage current mechanisms of the MPS are (i) thermionic emission, (ii) thermionic field emission, (iii) field emission, and (iv) generation in the depletion region. In addition to these basic mechanisms, surface leakage and defect-related leakage may occur. Practical devices contain current components caused by more than one of these mechanisms. The dominant mechanism depends on the Schottky barrier height, temperature, applied voltage, surface status, and defects in the material. Due to the wide bandgap of SiC, the component (iv) offers a very small fraction of the total leakage current. Here we consider only mechanisms (i), (ii) and (iii) in the present paper.

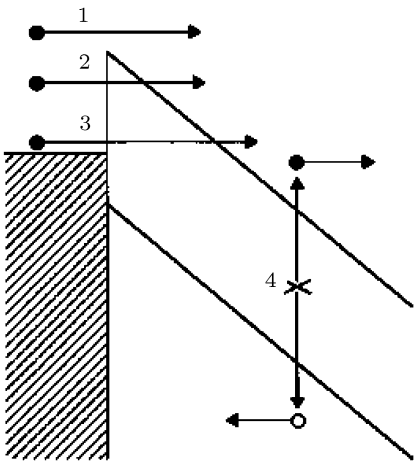


Fig.2. Basic reverse leakage current mechanisms of MPS diodes.

The thermionic emission reverse leakage current density depends on the Schottky barrier height and the temperature. Reverse leakage current density can be expressed as[9]

$$J_{\rm sch} \approx \left(\frac{S - X_j \bullet n}{W + S}\right) A^* T^2 \exp\left(-\frac{q(\phi_{\rm B} - \Delta\phi_{\rm B})}{kT}\right), \tag{1}$$

where T is the temperature, A^* is Richardson's constant, k is Boltzmann's constant, $\phi_{\rm B}$ is the Schottky barrier height and $\Delta\phi_{\rm B}$ is the lowering amount of image-force barrier height. The lowering of image-force barrier height reduces the effective Schottky barrier height by an amount that depends on the electric field at the Schottky contact as shown in the following expression[9]

$$\Delta\phi_{\rm B} = 2q\left(\frac{q\xi_{\rm s}}{16\pi\varepsilon_{\rm s}}\right)^{1/2}, \tag{2}$$

where $\xi_{\rm s}$ is the electric field at the Schottky contact.

Experimentally, the reverse leakage current of the 4H–SiC MPS Schottky diode has a larger magnitude than expected by thermionic emission and a stronger dependence than predicted by the lowering of image-force barrier height. So thermionic field emission and field emission must be considered, which are usually disregarded for the contribution to the inverse current. The tunnelling probability as a function of energy through a reverse bias Schottky barrier can be approximated using the WKB theory as shown in expressions (3) and (4)[10]

$$T(E) = 1 \quad \text{for} \quad E > E_{\rm B} - qV_{\rm R} + E_{\rm f}, \tag{3}$$

$$T(E) = \exp\left[\frac{2}{q\hbar}\sqrt{\frac{m^*\varepsilon_{\rm s}}{N_{\rm f}}}\left\{E\ln\left(\frac{\sqrt{E_{\rm B}-qV_{\rm R}+E_{\rm f}}+\sqrt{E_{\rm B}-qV_{\rm R}+E_{\rm f}-E}}{E}\right)\right.\right.$$
$$\left.\left.-\sqrt{E_{\rm B}-qV_{\rm R}+E_{\rm f}}(\sqrt{E_{\rm B}-qV_{\rm R}+E_{\rm f}-E})\right\}\right]$$
$$\text{for}\quad 0<E<E_{\rm B}-qV_{\rm R}+E_{\rm f}, \tag{4}$$

where $\hbar$ is Planck's constant, q is the electron charge, m^* is the tunnelling electron, $\varepsilon_{\rm s}$ is the 4H–SiC dielectric constant, $E_{\rm f}$ is the semiconductor Fermi energy, $E_{\rm B}$ is the Schottky barrier height, $V_{\rm R}$ is the applied bias, and $N_{\rm f}$ is the N^- epi-layer doping. So the tunnelling current density of the 4H–SiC MPS can be expressed as

$$J_{\rm T} = \left(\frac{S-X_j\bullet n}{W+S}\right)\left[\frac{qm^*k_{\rm B}T}{2\pi^2\hbar^3}\int_0^{E_{\rm B}-qV_{\rm R}+E_{\rm f}} T(E)K(E){\rm d}(E)+\int_{E_{\rm B}-qV_{\rm R}+E_{\rm f}}^{\infty} T(E)K(E){\rm d}(E)\right], \tag{5}$$

where S is the p-region space, W is the P-region width, n is the lateral diffusion ratio of the junction, X_j is the junction depth, and $K(T)$ is described as[10]

$$K(T) = \ln\{(1+\exp[(-E_{\rm f}-E)/k_{\rm B}T])(1+\exp[(-E_{\rm f}-E+V_{\rm R})/k_{\rm B}T])^{-1}\}. \tag{6}$$

The tunnelling probability is then inserted into expression (5) and integrated. Then relationship between tunnelling current density and electric field for the MPS can be written as

$$J_{\rm T} = \left(\frac{S-X_j\bullet n}{W+S}\right)\frac{q^2m_0\xi_{\rm s}}{16\pi^2\hbar m^*\phi_{\rm B}}\exp\left(-\frac{4(2m^*)^{1/2}(q\phi_{\rm B})^{3/2}}{3q\hbar\xi_{\rm s}}\right). \tag{7}$$

The appropriate transport effective mass can be calculated for the conduction in a given direction by using the components of the effective mass tensor, m_x, m_y, and m_z and the direction cosines l, m, n of the unit normal to the interface relative to the principal axes of the constant energy ellipsoid. The transport effective mass m^* can be described as

$$m^* = \sqrt{(l^2m_ym_z+m^2m_zm_x+n^2m_xm_y)}. \tag{8}$$

The theoretical tunnelling effective mass is calculated to be $0.33m_0$ for the current direction along the c-axis based on the previously reported effective mass tensor values for 4H–SiC.[11]

2.2. Electric field at the Schottky contact

Because the electric field in an MPS diode is in 2-D distribution, Poisson's equation in the cylindrical coordinate system is necessarily solved. The cell of the 4H–SiC MPS is shown in Fig.3. In an N^- depletion region, the cylindrical Poisson equation is

$$\frac{1}{r}\frac{\rm d}{{\rm d}r}\left[r\frac{{\rm d}V}{{\rm d}r}\right] = \frac{1}{r}\frac{\rm d}{{\rm d}r}(r\xi) = \frac{q\beta N_{\rm d}}{\varepsilon_{\rm s}}, \tag{9}$$

where ξ is the electric field, V is the voltage across the depletion region, $N_{\rm d}$ is the N^- epi-layer doping, β is the ionization rate of 4H–SiC in the N^- region, $\varepsilon_{\rm s}$ is the 4H–SiC dielectric constant. With the electric field boundary conditions at the depletion boundary that the voltage is zero, we can solve Eq.(7) and obtain the following expressions

$$\xi(r) = \frac{q\beta N_{\rm d}}{2\varepsilon_{\rm s}}\left[\frac{r_{\rm d}^2-r^2}{r}\right], \tag{10}$$

$$V = \frac{q\beta N_{\rm d}}{2\varepsilon_{\rm s}}\left[\frac{X_j^2-r^2}{2}+r_{\rm d}^2\ln\left(\frac{r_{\rm d}}{r_j}\right)\right]. \tag{11}$$

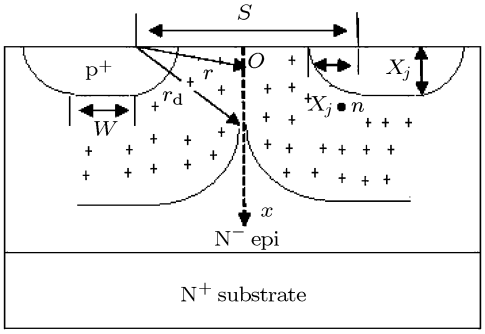


Fig.3. Cell of the MPS diode.

Assuming that the positive voltage applied to the N^+ substrate is $V_{\rm R}$, and substituting it into expression (11), we can find $r_{\rm d}$. By using $r_{\rm d}$ and the cylindrical

symmetric and electric field solution, the electric field along the x-axis can be written as

$$\xi(x) = 2\xi(r_{\mathrm{d}}) \times \sin(\alpha) = \frac{q\beta N_{\mathrm{d}}}{2\varepsilon_{\mathrm{s}}} \left[\frac{r_{\mathrm{d}}^2 - (s/2)^2 - x^2}{\sqrt{(s/2)^2 + x^2}} \right]. \quad (12)$$

At the point x_0 where $\mathrm{d}\xi(x)/\mathrm{d}x = 0$, the electric field along the x-axis reaches a maximum. The electric field at the Schottky contact, ξ_{s}, is approximately expressed as

$$\xi_{\mathrm{s}} = \xi(x_0) \approx \frac{q\beta N_{\mathrm{d}}}{\varepsilon_{\mathrm{s}}} \left[\frac{S^2}{4} \left(\frac{2\varepsilon_{\mathrm{s}} V_{\mathrm{R}} X_j}{q\beta N_{\mathrm{d}}} - \frac{X_j^3}{2} \right)^{2/3} \right]^{1/2}. \quad (13)$$

The electric field at the Schottky contact is calculated from Eq.(13) and plotted together with the DESSIS-ISE software simulation results in Fig.4, which shows that both are in good agreement. It shows that with smaller S, the electric field at the Schottky contact is more efficiently reduced in the MPS. Another factor to affect the electric field at the Schottky contact is the P junction depth. The deeper the P junction depth is, the lower the electric field formed at the Schottky contact will be. These results are helpful for optimizing the design of the high voltage MPS diodes.

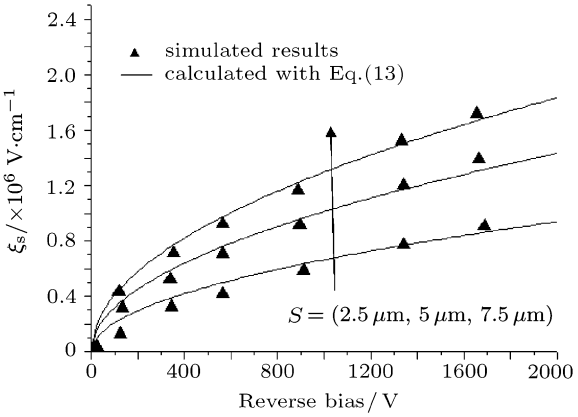


Fig.4. Simulated and calculated relations between the electric field at the Schottky contact and the reverse bias at different P-region spacings.

3. Results and discussion

Figure 5 shows a comparison between calculated reverse leakage currents with experimental results[4] of the 4H–SiC MPS. At a low voltage bias, the leakage current is dominated by thermionic emission. The experimental data are several orders of magnitude higher than the calculated results because the minimum value that the testing setup can measure is about $\sim 10^{-10}$ A.[8] The barrier height used in the calculations is 1.3 V, which was measured by using the C–V technique.[5] It can be seen in Fig.5 that the calculated results show good agreement with the experimental results at high reverse voltages. This confirms that the leakage current is dominated by the tunnelling current at high reverse voltages and the accuracy of our analytical model. In addition, it can also be seen that the experimental results are a little bigger than the calculated results at high reverse voltages. We speculate that this discrepancy arises partly from the presence of the edge leakage current caused by the higher electric fields at the edge.

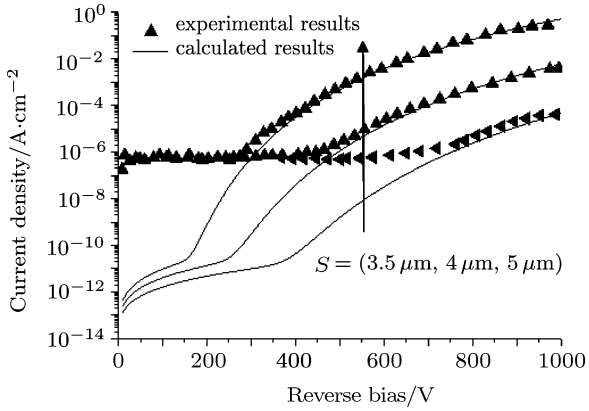


Fig.5. Calculated and measured reverse characteristics of the 4H–SiC MPS diode at 23 °C.

4. Summary

A new analytical model for the reverse characteristics of 4H–SiC merged PN–Schottky diodes (MPS) is developed in this paper. By solving the cylindrical Poisson equation and utilizing the WKB approach, an accurate model of the electric field at the Schottky contact and a reverse current density model of MPS are proposed. The electric fields at the Schottky contact match the simulation results from the ISE simulator and the calculated results of the reverse current densities of SiC MPS show good agreement with the experimental data. This confirms that the leakage current is dominated by the tunnelling current at high reverse voltages.

References

[1] Callanan R J, Aqarwal A and Burk A 2008 34^{th} *Annual Conference of IEEE* **2885–2890**

[2] Yang L A, Zhang Y M, Yu C L and Zhang Y M 2003 *Acta Phys. Sin.* **52** 302 (in Chinese)

[3] Kim S C and Wook B H 2008 *Proc. 26th Int. Conf. on Microelectronics* **181–184**

[4] Zhao J H, Alexandrow P, Fursin L, Feng Z C and Weiner M 2002 *Electron. Lett.* **38** 1389

[5] Zhu L, Chow T P, AJones K and Agarwal A 2006 *IEEE Trans. Electron Devices* **53** 363

[6] Chow T P 2000 *Silicon Carbide Power Devices* (New York: Academic) **249–298**

[7] Baliga B J 1985 *Solid State Electron* **28** 1089

[8] Zhu L and Paul T 2008 *Transactions on Electron Devices* **55** 1857

[9] Schoen K J, Woodall J M and Cooper A 1998 *IEEE Trans Electron Devices* **45** 1595

[10] Crofton J and Sriram S *IEEE Trans. on Electron Device* **43** 2305

[11] Person C and Lindefelt U 1999 *J. Appl. Phys.* **86** 5036